Electronic Skin with Energy Autonomous Proximity Sensing for Human-Robot Interaction

Pablo Escobedo, Markellos Ntagios and Ravinder Dahiya, *Fellow, IEEE*
Bendable Electronics and Sensing Technologies (BEST), University of Glasgow, Glasgow, UK, G12 8QQ
Correspondence to - Ravinder.Dahiya@glasgow.ac.uk

***Abstract*—Electronic skin or eSkin is critical to enhance the interactive capabilities of robots through physical contact. The current approaches to develop this capability involve using multiple sensors distributed on robot's body. Energy requirement of such eSkin is currently met through batteries, which is not ideal as it may reduce the operational time and requires frequent charging. In this work, we present an eSkin consisting of distributed energy autonomous proximity sensors. The eSkin contains an array of miniaturized solar cells to generate energy needed for infrared LEDs based proximity sensors. As a proof of concept, the eSkin has been integrated in an industrial robot arm UR5 and proximity sensing has been shown to enable safe Human-Robot Interaction (HRI).**

Keywords— Electronic Skin, Energy Autonomy, Human-Robot Interaction, Proximity sensing

I. Introduction

Electronic skin or eSkin has recently emerged as a novel platform for advances in robotics, prosthesis, health diagnostics, therapeutics, and monitoring [1]. It allows robots and prosthetic limbs to gather information from large areas and to exploit it to operate in unstructured environments or to improve human-robot interaction [2]–[6]. The conventional approach requires rigorous distributed sensor designs [7]–[9], circuits and power supply [8], [10]. A robust and steady power source is needed for next-generation smart, stand-alone, active eSkin systems. This remains a challenge as the continuous power supply through batteries is not a practical solution as they add weight, are not flexible, and may require redesigning of robotics platforms [11], [12]. Various strategies developed so far shown to address the energy autonomy issue have focused on either minimizing the power through low-power electronics [13], [14] power-management circuits or by using various types of energy harvesters [8], [11], [15]–[18]. By using a combination of these, recently energy autonomous sensors have been explored.

Among various sensing modalities for eSkin, the proximity sensing is a crucial element for the safe operation of robots. Proximity sensing holds the key for robots to react swiftly to avoid collision with an object coming in its workspace during operation [19]. The proximity sensing is crucial element for safe operation of robots [20], [21], particularly in industry settings where human and robots are expected to share the workspace. For proximity sensing, many approaches have been used in past. These include sensors based on infrared (IR), ultrasonics, or lasers [21]. Most of the reported optical proximity sensors have been designed to perform in a non-contact mode which sends the signals to robotic control unit to prevent collisions.

Herein we present a new approach, whereby an eSkin, comprising of an array of solar cells, powers the distributed proximity sensors [22]. The eSkin is integrated on a 3D-printed robotic hand. The sensing system consists of discrete Si photovoltaic (PV) cells integrated on soft and flexible polydimethylsiloxane (PDMS) substrate for conformable coverage over curved surfaces. The PV cells generate the power required to operate the proximity sensors under different illumination conditions. To achieve proximity sensing, the eSkin uses the infrared light reflection produced by IR LEDs between the eSkin and a surrounding object. The developed skin shows the continuous power generation in the range of ~10 mW/cm^2 considering the whole array of solar cells distributed in the palm area. The approach presented here also shows that, when it comes to engineered solution, the distribution of sensors on large areas (as in human skin) is not a problem or hurdle to deal with. Instead it is an opportunity to generate power and develop energy autonomous robots.

This paper is organised as follows: Various materials and methods used for the development of eSkin with energy autonomous proximity sensors are presented in Section II. A detailed discussed about the experimental results in given in Section III and the key outcomes are summarised in Section IV.

II. Materials and Methods

The solar eSkin system comprises of the following blocks: *(i)* distributed array of miniaturized PV cells and IR LEDs; *(ii)* the driver and readout electronics; (*iii)* digital processing and communication interface; and *(iv)* power management system .

A. Solar eSkin design and fabrication

The solar cells used are commercially available (Pmaxx™ Series, Silicon Solar, New York, USA) monocrystalline PV cells with an open-circuit voltage (V_{OC}) of 0.55 V and a short-circuit current (I_{SC}) of 100 mA. The PV cells had an initial size of 7.8 cm^2, they were diced using a laser engraving machine model Speedy 300 (Trotec Laser, Marchtrenk, Austria) to obtain 1 cm^2 size cells. The resulting small sized solar cells were distributed in an array of 25 cells, which was placed as a proof of concept on the palm of a 3D-printed robotic hand (Fig. 1). Soft and flexible polydimethylsiloxane (PDMS) was used as the supporting substrate for the PV cells array. The PDMS layer was prepared through three stages: *(i)* mixing of silicone elastomer and curing agent (Sigma Aldrich); *(ii)* degassing and removal of trapped air bubbles; and *(iii)* curing at 60ºC for 3 hrs [23], [24].

B. *Readout circuit design and fabrication*

The core of the driver and readout electronics is a 32-bit Arm Cortex®-M3 microcontroller (MCU) model LPC1768 (NXP Semiconductors, Eindhoven, The Netherlands). Pulse width modulator (PWM) outputs were used to drive the IR LEDs at a fixed frequency of 20 kHz and 50% duty cycle. The LEDs included in the eSkin were IR emitting diodes using GaAlAs multi-quantum well (MQW) technology model TSML1020 (Vishay Semiconductors, Pennsylvania, USA) with peak emission at 940 nm. The output of each PWM module was connected to a silicon n-MOSFET with low on-resistance and fast switching speed (2SK3541T2L, ROHM Semiconductor, Kyoto, Japan). Each IR LED was connected in series with a 330 Ω between the supply and the drain terminal of each n-MOSFET. Each solar cell in the eSkin was connected to an input of a 32-channel analog multiplexer model ADG732 (Analog Devices, Massachusetts, USA), whose output channel was controlled by the MCU.

Various stages required for signal acquisition are depicted in Fig 1. In summary, the output current is converted to voltage through a I-V conversion stage, after which the offset component of the signal is removed using a DC blocking capacitor. After this, the signal will be a sinusoidal waveform whose frequency is equal to the frequency of the square signal at which the IR LEDs are driven, i.e., 20 kHz. The amplitude of the signal increases as the object approaches the eSkin, meaning that more radiation is being reflected back to the solar cell. Therefore, the AC signal is rectified and filtered to obtain a constant voltage value at the output of the readout electronics. This is done by a half-wave precision rectifier based on the OPA177 operational amplifier. The resulting signal is then converted from analog to digital domain through the 12-bit ADC input of the MCU. Finally, the reading is digitally processed and prepared for visualization in the PC. By using this configuration, the variations in cells' output current, caused by the reflected radiation from the IR LEDs, are converted to the rectified voltage whose amplitude is related to the distance of the object that reflects the IR radiation.

C. *Communication interface and digital processing*

LabVIEW 2018 Robotics v18.0f2 (National Instruments, Texas, USA) was used as a graphical programming interface for the digital processing and visualization of data coming from the solar eSkin. The MCU connects to a PC running LabVIEW by means of a USB interface. The raw data digitalized by the 12-bit ADC integrated in the MCU is transmitted to the PC using serial communication with a baud rate of 9600 bps. To mitigate the effects of noise and errors due to serial communication, the raw data was filtered within the LabVIEW program. Firstly, the signal was smoothed using a median filter with the rank set to 2. The filtered data then went through a moving average filter with a sample length set to 50, which was experimentally found to be a good trade-off between noise reduction and processing speed.

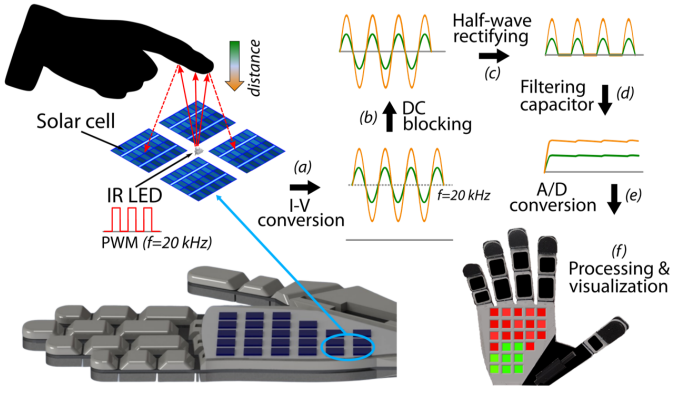

Fig. 1. Working principle of proximity sensing in the solar eSkin system.

D. *3D printed robotic hand*

The robotic hand and wrist were designed with the Computer-Aided-Design (CAD) software SolidWorks 2018 SP4.0 (Dassault Systems, Vélizy-Villacoublay, France). They were printed with Ultimaker S5 3D printer using Polylactic acid (PLA, RS Components). More details can be found in our previous publications [25], [26].

III. Results and Discussion

A. *Energy generation and management*

The PV cells in the distributed array were connected in parallel branches. The output of the array of PV cells was connected to a micro-power, high-efficiency solar power management module ISV019V1 (STMicroelectronics, Geneva, Switzerland), which is based on the SPV1050 integrated circuit from the same manufacturer. The SPV1050 is an ultra-low power energy harvester with an embedded Maximum Power Point Tracking (MPPT) algorithm, a battery charger and a power manager. It integrates a DC-DC converter stage that was configured as boost, providing a regulated output voltage of 3.3 V. By enabling the MPPT feature, the SPV1050 regulates the working point of the DC-DC converter by tracking its output voltage so that $V_{IN} = V_{MPP}$, thus maximizing the power extracted from the source. In our case, the driver and readout electronics consumption were 23.9 mA at 3.3 V (78.9 mW) without considering the MCU. In active mode and at the maximum operating frequency of 100 MHz, the LPC1768 MCU consumed a total power of 155 mW (47 mA at 3.3 V) according to the specifications, considering not only the power consumption of the MCU but also the consumption of all used peripherals (UART, PWM and ADC modules). As per the power consumption of the IR LEDs used as proximity sensors, each one draws 16.5 mW (10 mA at 3.3 V at a 50% duty cycle). For the proof of concept, 4 IR LEDs were included in some intersection points of the solar eSkin, making a total of 66 mW. Thanks to the MPPT feature of the used solar power manager, we can consider that the cells will be working close to the MPP point under adequate light conditions. The light source used in this study is a 4 W LED lamp with color temperature (CCT) of 4500 K and Color Rendering Index (CRI) higher than 80 RA (LT-T15, Aglaia, California, USA). This device generates a white light with an intensity of 650 Lux at a distance of 35 cm. If all cells in the palm of the robotic hand were working on the MPP measured with such light source, the presented skin would generate more than twice the power required for the system operation in active mode at the highest clock rate of 100 MHz. However, there can be some scenarios where the system will not

TABLE I

POWER BUDGET: SUMMARY OF THE SURPLUS POWER GENERATED AFTER CONSIDERING GENERATION AND CONSUMPTION OF THE SOLAR ESKIN.

System	Conditions	Surplus Power (mW)
Solar eSkin powered by palm solar cells	100 MHz, all palm cells at MPP	317.6
	100 MHz, 50% of cells at MPP	8.75
	12 MHz, all palm cells at MPP	435.7
	12 MHz, 50% of palm cells at MPP	127.0
	12 MHz, 30% of palm cells at MPP	3.50

operate under these ideal conditions, i.e., all the cells will not be illuminated all the time to allow the maximum power generation. In such cases, considering the maximum power required (~300 mW), we would be able to operate the system using 50% of the solar cells in the palm of the robotic hand working at the MPP. If we operate the system at the slower clock rate of 12 MHz, 30% of the solar cells would be needed at MPP to fulfill the power requirements of the system. In any case, the surplus energy generated under adequate light conditions could be used to charge a battery through the solar power management module based on the SPV1050 chip. Table I shows the net power generated after considering generation and consumption under different conditions.

B. *Proximity sensing*

The operation of the proximity sensing was based on recording the reflection of infrared radiation from the IR LEDs when it bounces off an object approaching the eSkin (Fig 1). In such scenario, the amount of reflection going back to the solar cells will have an influence on their output current. When properly acquired by the readout electronics and processed by digital filtering (see Section II), a calibration curve of output voltage as a function of distance can be obtained, as shown in Fig 2.

The eSkin could provide the robotic hands with proximity or soft touch feedback for smarter reaction capabilities needed for object collision avoidance and safe human-robot interaction (HRI) [27]. To this end, we have integrated the eSkin on 3D-printed hand on an industrial robot arm UR5 (Universal Robots,

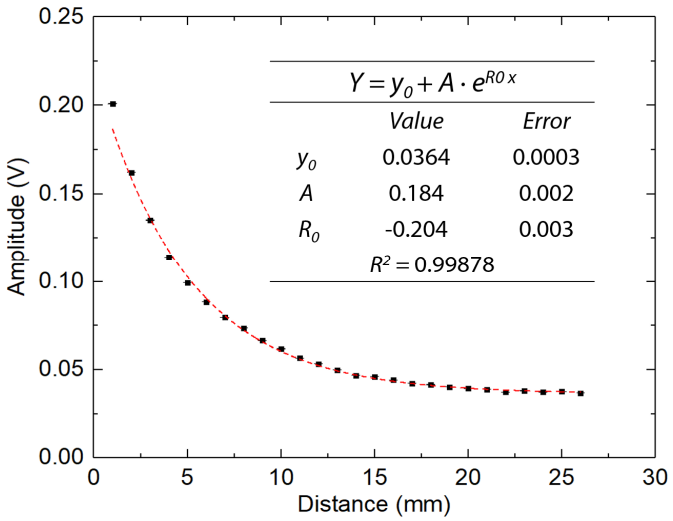

Fig. 2. Voltage versus distance between the approaching object and the eSkin using the output of a single solar cell under environmental lighting conditions.

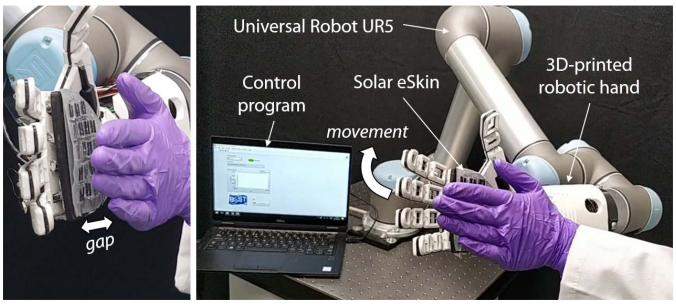

Fig. 3. Solar eSkin integrated with a Universal Robot UR5 for safe HRI.

Odense, Denmark). LabVIEW 2018 Robotics (National Instruments, Texas, USA) program was used to control the movements (using real-time proximity sensing mode) of the UR5 in response to an object approaching the solar eSkin. The system is shown in Fig. 3, where the eSkin detects the approaching a human hand and enable the UR5 robot arm to react immediately by moving away to avoid a collision.

IV. CONCLUSIONS

In this work, the operating principle of solar cells is harnessed for energy autonomous sensing. The solar cells on the eSkin harvest the energy needed to power the IRLEDs based proximity sensors. Using this approach, a large area flexible and conformable eSkin has been developed with distributed miniaturized solar cells in a matrix. As a proof of concept, the developed solar eSkin was integrated into a custom-designed 3D-printed robotic hand. Under adequate light conditions, the readout electronics and sensors can be powered by the energy generated by the solar eSkin itself, thus becoming an energy autonomous system. In fact, the surplus of energy can be stored in batteries as a backup for later use when the light conditions are not good enough. A further step was taken by integrating the 3D-printed hand with solar eSkin onto an industrial robot arm UR5 from Universal Robots. The real-time closed control loop implemented to endow the robot arm with reaction capability shows the eSkin operating effectively in proximity sensing mode to prevent collisions of robotic hand with approaching objects or individuals, thus opening a promising route for safe HRI. Future work will involve whole body implementation of the presented eSkin, possibly with different type of sensors.

ACKNOWLEDGMENT

This work is supported in part by Engineering and Physical Sciences Research Council (EPSRC) through engineering fellowship for growth (EP/R029644/1 and EP/M002527/1) and North West Centre for Advanced Manufacturing (NW CAM) project supported by the European Union's INTERREG VA Programme (H2020-Intereg-IVA5055), managed by the Special EU Programmes Body (SEUPB). The views and opinions in this document do not necessarily reflect those of the European Commission or the Special EU Programmes Body (SEUPB).

REFERENCES

[1] R. Dahiya, "E-Skin: From Humanoids to Humans [Point of View]," *Proc. IEEE*, vol. 107, no. 2, pp. 247–252, Feb. 2019.

[2] T. Belpaeme, J. Kennedy, A. Ramachandran, B. Scassellati, and F. Tanaka, "Social robots for education: A review," *Sci. Robot.*, vol. 3, no. 21, Aug. 2018.

[3] I. Leite, C. Martinho, and A. Paiva, "Social Robots for Long-Term Interaction: A Survey," *Int. J. Soc. Robot.*, vol. 5, no. 2, pp. 291–308, Apr. 2013.

[4] R. S. Dahiya and M. Valle, *Robotic Tactile Sensing: Technologies and System*. Dordrecht: Springer, 2013.

[5] B. D. Argall and A. G. Billard, "A survey of Tactile Human–Robot Interactions," *Rob. Auton. Syst.*, vol. 58, no. 10, pp. 1159–1176, Oct. 2010.

[6] T. Yamaguchi, T. Kashiwagi, T. Arie, S. Akita, and K. Takei, "Human□Like Electronic Skin□Integrated Soft Robotic Hand," *Adv. Intell. Syst.*, vol. 1, no. 2, p. 1900018, Jun. 2019.

[7] C. Zhang, S. Liu, X. Huang, W. Guo, Y. Li, and H. Wu, "A stretchable dual-mode sensor array for multifunctional robotic electronic skin," *Nano Energy*, vol. 62, no. March, pp. 164–170, 2019.

[8] R. Dahiya *et al.*, "Large-Area Soft e-Skin: The Challenges Beyond Sensor Designs," *Proc. IEEE*, vol. 107, no. 10, pp. 2016–2033, Oct. 2019.

[9] S. Baek *et al.*, "Flexible piezocapacitive sensors based on wrinkled microstructures: Toward low-cost fabrication of pressure sensors over large areas," *RSC Adv.*, vol. 7, no. 63, pp. 39420–39426, 2017.

[10] R. D. I. G. Dharmasena *et al.*, "Energy Scavenging and Powering E-Skin Functional Devices," *Proc. IEEE*, vol. 107, no. 10, pp. 2118–2136, 2019.

[11] C. García Núñez, L. Manjakkal, and R. Dahiya, "Energy autonomous electronic skin," *npj Flex. Electron.*, vol. 3, no. 1, p. 1, Dec. 2019.

[12] L. Manjakkal, C. G. Núñez, W. Dang, and R. Dahiya, "Flexible self-charging supercapacitor based on graphene-Ag-3D graphene foam electrodes," *Nano Energy*, vol. 51, no. March, pp. 604–612, Sep. 2018.

[13] C. Jiang, H. W. Choi, X. Cheng, H. Ma, D. Hasko, and A. Nathan, "Printed subthreshold organic transistors operating at high gain and ultralow power," *Science (80-.).*, vol. 363, no. 6428, pp. 719–723, Feb. 2019.

[14] C. Jiang, X. Cheng, and A. Nathan, "Flexible Ultralow-Power Sensor Interfaces for E-Skin," *Proc. IEEE*, vol. 107, no. 10, pp. 2084–2105, Oct. 2019.

[15] R. Dahiya, D. Akinwande, and J. S. Chang, "Flexible Electronic Skin: From Humanoids to Humans [Scanning the Issue]," *Proc. IEEE*, vol. 107, no. 10, pp. 2011–2015, Oct. 2019.

[16] K. Yu, S. Rich, S. Lee, K. Fukuda, T. Yokota, and T. Someya, "Organic Photovoltaics: Toward Self-Powered Wearable Electronics," *Proc. IEEE*, vol. 107, no. 10, pp. 2137–2154, Oct. 2019.

[17] G. Min, L. Manjakkal, D. M. Mulvihill, and R. S. Dahiya, "Triboelectric Nanogenerator with Enhanced Performance via an Optimized Low Permittivity Substrate," *IEEE Sens. J.*, vol. PP, no. c, pp. 1–1, 2019.

[18] P. Escobedo, I. M. P. de Vargas-Sansalvador, M. Carvajal, L. F. Capitán-Vallvey, A. J. Palma, and A. Martínez-Olmos, "Flexible passive tag based on light energy harvesting for gas threshold determination in sealed environments," *Sensors Actuators B Chem.*, vol. 236, pp. 226–232, Nov. 2016.

[19] K. K. Sadasivuni, A. Kafy, L. Zhai, H. U. Ko, S. Mun, and J. Kim, "Transparent and flexible cellulose nanocrystal/reduced graphene oxide film for proximity sensing," *Small*, vol. 11, no. 8, pp. 994–1002, 2015.

[20] K. K. Sadasivuni, A. Kafy, L. Zhai, H.-U. Ko, S. Mun, and J. Kim, "Transparent and Flexible Cellulose Nanocrystal/Reduced Graphene Oxide Film for Proximity Sensing," *Small*, vol. 11, no. 8, pp. 994–1002, Feb. 2015.

[21] V. J. Lumelsky, M. S. Shur, and S. Wagner, "Sensitive skin," *IEEE Sens. J.*, vol. 1, no. 1, pp. 41–51, Jun. 2001.

[22] P. Escobedo, M. Ntagios, D. Shakthivel, W. Navaraj, and R. Dahiya, "Energy Generating Electronic Skin with Intrinsic Tactile Sensing without Touch Sensors," *IEEE Trans. Robot.*, 2020.

[23] S. Gupta, A. Vilouras, and R. Dahiya, "Polydimethylsiloxane as polymeric protective coating for fabrication of ultra-thin chips," *Microelectron. Eng.*, vol. 301, p. 111157, Oct. 2019.

[24] R. Dahiya, G. Gottardi, and N. Laidani, "PDMS residues-free micro/macrostructures on flexible substrates," *Microelectron. Eng.*, vol. 136, pp. 57–62, Mar. 2015.

[25] M. Ntagios, H. Nassar, A. Pullanchiyodan, W. T. Navaraj, and R. Dahiya, "Robotic Hands with Intrinsic Tactile Sensing via 3D Printed Soft Pressure Sensors," *Adv. Intell. Syst.*, p. 1900080, 2019.

[26] W. Navaraj and R. Dahiya, "Fingerprint□Enhanced Capacitive□ Piezoelectric Flexible Sensing Skin to Discriminate Static and Dynamic Tactile Stimuli," *Adv. Intell. Syst.*, vol. 1900051, p. 1900051, Sep. 2019.

[27] P. A. Lasota, T. Fong, and J. A. Shah, "A Survey of Methods for Safe Human-Robot Interaction," *Found. Trends Robot.*, vol. 5, no. 3, pp. 261–349, 2017.